

CHEMPHYSICHEM

Supporting Information

© Copyright Wiley-VCH Verlag GmbH & Co. KGaA, 69451 Weinheim, 2013

Top-Hat and Asymmetric Gaussian-Based Fitting Functions for Quantifying Directional Single-Molecule Motion

David J. Rowland and Julie S. Biteen^{*[a]}

cphc_201300774_sm_miscellaneous_information.pdf
cphc_201300774_sm_a.avi

Supporting Information for: Asymmetric Gaussian and Top-Hat Based Fitting Functions for Quantifying Directional Single-Molecule Motion

David Rowland^[a], Julie S. Biteen^{[a]*}

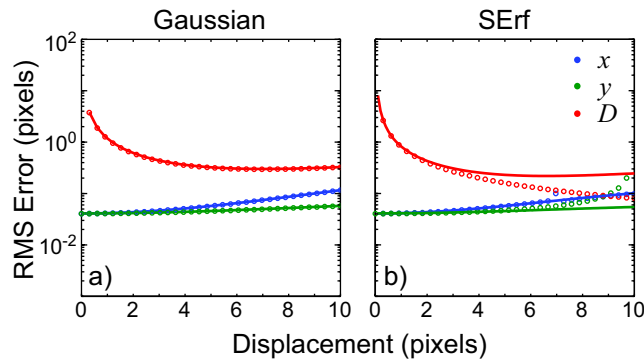
^[a]University of Michigan Department of Chemistry, Ann Arbor, MI 48109, USA

*Correspondence should be addressed to jsbiteen@umich.edu

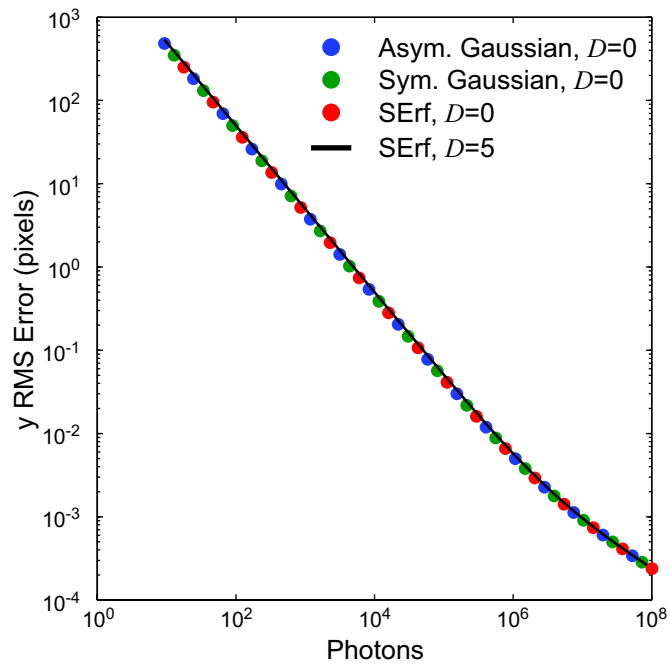
Supporting Movie 1:

Cellular_Motion-7by5um-10fps.avi

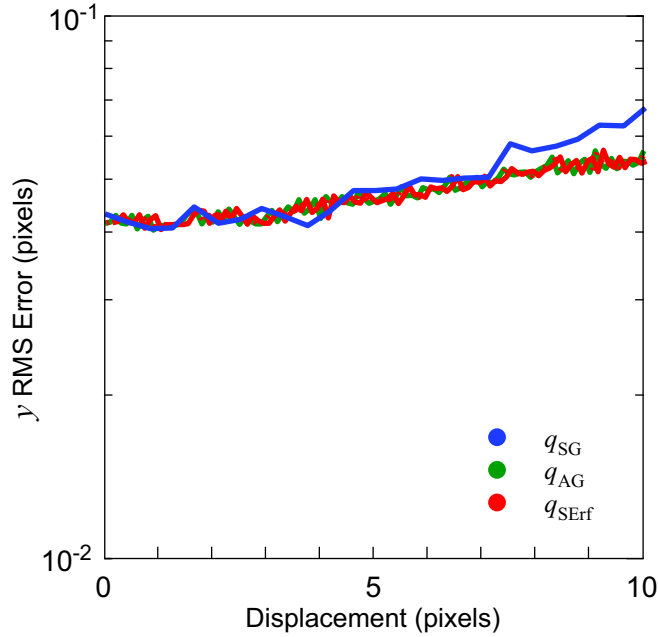
Antibody-labeled *Vibrio cholerae* cell imaged under 488-nm excitation at a 10 Hz frame rate. Viewing region: 7.056 μm by 5.145 μm .



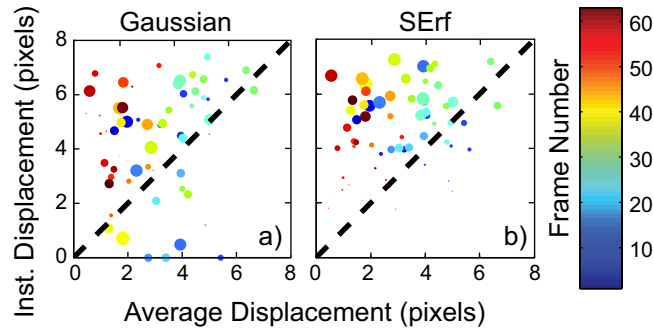
Supporting Figure 1: Precision for x , y , and D computed using Fisher information theory. Solid lines: numerical solutions to the integrals in Equation (5); circles: approximate closed-form analytical solutions from Table 1. Here, $N = 1 \times 10^5$ pixels, $b = 200$ photons/pixel, $\phi = 0$ and $\sigma = 2$ pixels.



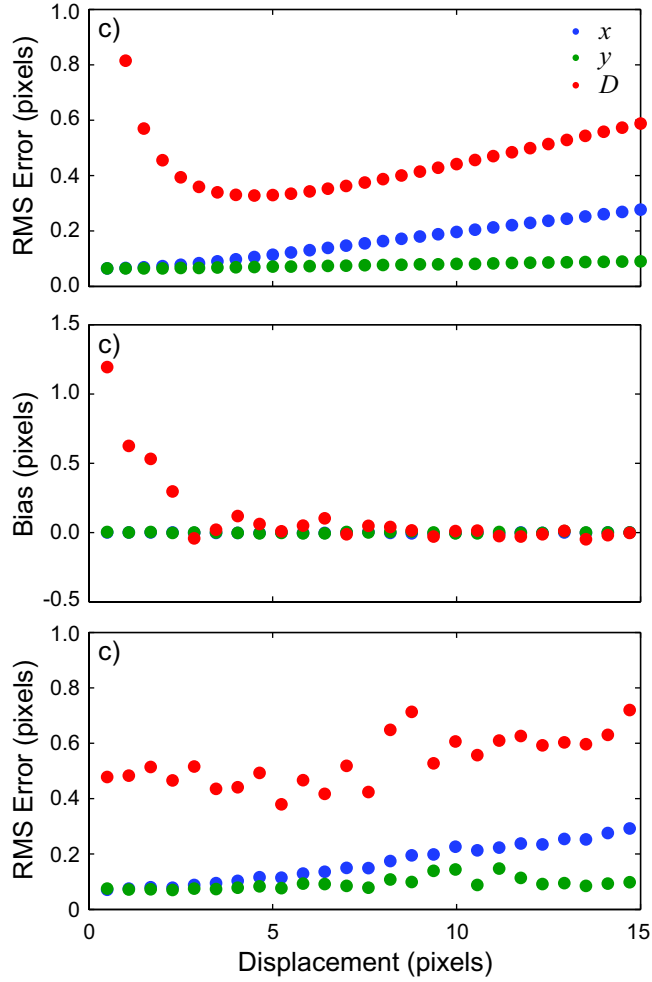
Supporting Figure 2: Comparison of precision in y (perpendicular to the direction of motion) calculated from Fisher information, based on using the symmetric Gaussian, asymmetric Gaussian and SErf fitting functions (dotted green, blue and red lines, respectively) for estimating the position of an *immobile* particle. The three functions all have the same performance. Solid black line: localization precision in y for fitting a *mobile* molecule ($D = 5$ pixels) with the SErf function; Δy for mobile particles converges at high photon count with Δy for the immobile particles.



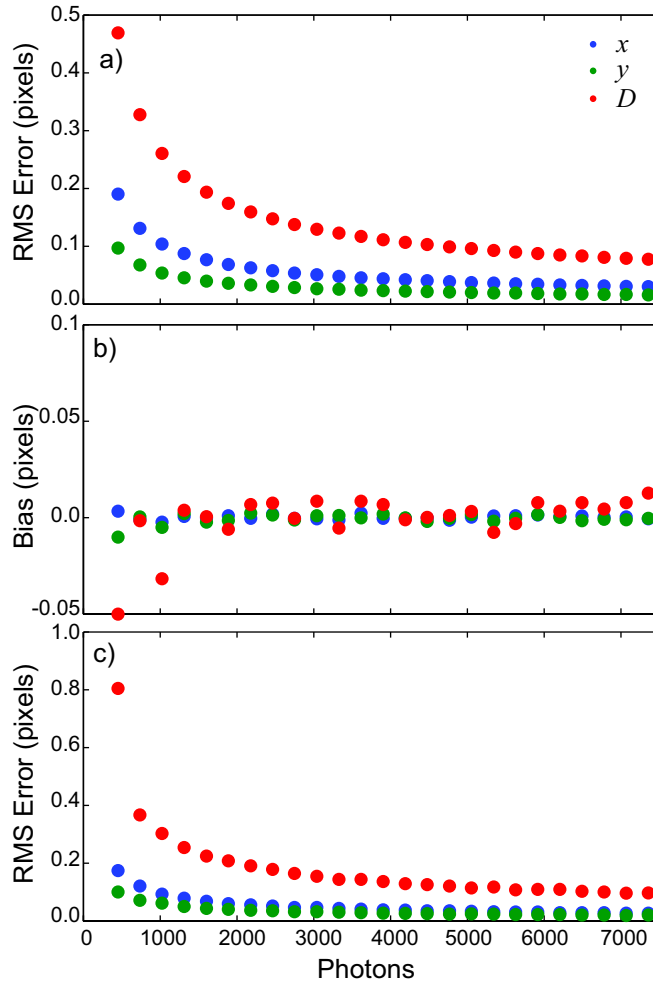
Supporting Figure 3: Comparison of symmetric, asymmetric and SErf fitting functions (blue, green and red lines, respectively) for fitting a mobile particle. As in-frame displacement, D , increases, the asymmetric Gaussian and SErf functions (q_{AG} and q_{SErf} , respectively), begin to outperform the symmetric Gaussian (q_{SG}).



Supporting Figure 4: Analysis of experimental images of a *Vibrio cholerae* cell in motion. Comparison of instantaneous displacement, D , from a fit to (a) the asymmetric Gaussian function ($c = 0.0104$) and (b) the SErf function, to average direction of motion, from the center-to-center average displacement over three-frame segments. The dashed lines show perfect correspondence, the color scale indicates the frame number, and the size of the points is inversely related to the square of the 95% confidence interval for the fit to the angle, ϕ .



Supporting Figure 5: Extension of the SErf fitting function analysis to the low photon count, low noise regime. (a) Precision for x , y , and D computed using numerical solutions to the Fisher information integrals. (b) Bias in estimation of x , y , and D from fitting simulated data. (c) Precision for x , y , and D from variance of fits to 1000 simulated images. Here, $b = 4$ photons/pixel, $N = 750$ photons, and $\sigma = 1.2$ pixels.



Supporting Figure 6: Extension of the SErf fitting function analysis to the low photon count, low noise regime. (a) Precision for x , y , and D computed using numerical solutions to the Fisher information integrals. (b) Bias in estimation of x , y , and D from fitting simulated data. (c) Precision for x , y , and D from variance of fits to 1000 simulated images. Here, b increases linearly with N from 3 to 12 photons/pixel, $\sigma = 1.2$ pixels, and $D = 7$ pixels.